Whiskerbot: A Robotic Active Touch System Modeled on the Rat Whisker Sensory System

Martin J. Pearson[1], Anthony G. Pipe[1], Chris Melhuish[1], Ben Mitchinson[2], Tony J. Prescott[2]

[1]*Bristol Robotics Laboratory, University of the West of England and University of Bristol, UK*

[2]*Adaptive Behaviour Research Group, Psychology Department, Sheffield University, UK*

The Whiskerbot project is a collaborative project between robotics engineers, computational neuroscientists and ethologists, aiming to build a biologically inspired robotic implementation of the rodent whisker sensory system. The morphology and mechanics of the large whiskers (macro-vibrissae) have been modeled, as have the neural structures that constitute the rodent central nervous system responsible for macro-vibrissae sensory processing. There are two principal motivations for this project. First, by implementing an artificial whisker sensory system controlled using biologically plausible neural networks we hope to test existing models more thoroughly and develop new hypotheses for vibrissal sensory processing. Second, the sensory mode of tactile whiskers could be useful for general mobile robotic sensory deployment. In this article the robotic platform that has been built is detailed as well as some of the experiments that have been conducted to test the neural control algorithms and architectures inspired from neuroethological observations to mediate adaptive behaviors.

1 Introduction

The rodents' use of their facial whiskers, or vibrissae, allows them to occupy visually occluded and physically confined environments. Few predators can operate effectively in such places, making the rodent family one of the most prolific and adaptable species on Earth. Ethological studies of rats' use of their vibrissae has highlighted many of the interesting behavioral attributes of this sensory modality (Ahl, 1986; Gustafson & Felbain-Keramidas, 1977; Vincent, 1912). The larger, more caudal vibrissae, or macro-vibrissae, are actively moved back and forth in a regular sweeping pattern, referred to as whisking, which has been postulated as highly instrumental in extracting spatial and textural information from the immediate sensory environment (Welker, 1964). When one or more vibrissae make contact with objects the rat tends to orient its snout towards the point of contact and dab the shorter, more rostral-ventral vibrissae (micro-vibrissae) upon the obstruction using small neck movements. In other situations rats have been observed using their macro-vibrissae to derive navigational cues such as wall following or tunnel running (Krupa, Matell, Brisben, Oliveira, & Nicole-

Correspondence to: Martin J. Pearson, Bristol Robotics Laboratory, University of the West of England and University of Bristol, DuPont Building, Coldharbour Lane, Bristol, BS16 1QY, UK.
E-mail: martin.pearson@brl.ac.uk
Tel.: +44 (0) 117 328 6321

lis, 2001; Milani, Steiner, & Huston, 1989). Further experiments have demonstrated that the macro-vibrissae can also discriminate surface textural detail (Carvell & Simons, 1990).

The superior colliculus is a neural structure within the brain which, in primates, is instrumental in rapidly orientating the fovea of the eye towards interesting stimuli detected in the head-centric visual field (Dean, Redgrave, & Westby, 1989). This same structure, in rodents, also has strong neural projections from the vibrissae sensory afferents (Killackey & Erzurumula, 2004) and has been shown to be employed for a similar orienting behavior (Benedetti, 1995). The snout tip is to the vibrissal system, what the retinal fovea is to the visual system; it is that part of the sensory apparatus with the greatest density of receptors. Hence head and neck movements, commanded by the colliculus, can bring this tactile "fovea" to bear on objects detected in the vibrissal field, just as collicular-generated saccades direct the eyes toward visual targets of interest (Di Scala, Schmitt, & Karli, 1983). In previous studies we have developed spiking neuron and population based neural models of the sensory processing pathways of the rat, including the superior colliculus and basal ganglia (Gurney, Prescott, & Redgrave, 2001; Mitchinson, Pearson, Melhuish, & Prescott, 2006). These models can be tuned to match empirical measurements taken from electrophysiology and have been integrated to generate simulated ethologically plausible animal behaviors.

Neurophysiological study has found that there is a topographically preserved representation of the vibrissae on the face of the animal in the somatosensory cortex of the brain (Woolsey & Van der Loos, 1970). The concentrated clusters of neurons in the somatosensory cortex, representing each vibrissa, are referred to as barrels and there are similarly represented neural concentrations found in the other major nuclei of the sensory pathway, namely barreloids in the thalamus (Van der Loos, 1976) and barrelettes in the trigeminal sensory complex (Ma, 1991). This topographic preservation provides an unprecedented amount of control when taking electrophysiological measurements at the different stages of the sensory pathway. The data can be used to elicit the processing roles of various neural structures and gain further insight into more generic sensory processing mechanisms.

Implementing and testing these models on a situated, embodied robotic platform is advantageous for three reasons. Firstly, the robustness of the models can be evaluated more thoroughly as they are exposed to real-time, noisy sensory stimuli. Secondly, real-world problems that the animal must overcome will be exposed by attempting to build such a platform. This will motivate further biological study to find out how the animal overcomes these problems and perhaps be guided by the engineering solutions that the roboticists employ. Thirdly, a tactile sensory modality based on the biology and neurology of mammalian whiskers would be useful for general mobile robotic deployment. Whiskers do not need to illuminate their environment to detect it as do more conventional sensors such as active IR, active ultrasonics, radar or vision. Therefore they can operate effectively in confined, noisy and visually occluded spaces, such as collapsed buildings or mine shafts, where conventional sensors become very unreliable. Not having to illuminate the environment also means that this sensory mode can be operated covertly, a property that may be of use for security or military requirements. Further to these potential applications, is the tolerance of the neural processing behind the physical whisker array to damage of the vibrissae (due to the sensors effectively remaining internal to the animal) and the observed ability to adapt to dramatic alterations of their physical morphology (Milani et al., 1989). This natural adaptability and robustness means that an artificial reproduction of this system could be exploited in situations in which immediate maintenance is not possible, such as planetary exploration or deep sea recovery (Hartmann, 2001). The work detailed in this report differs from other robotic whisker projects (Fend, Bovet, Yokoi, & Pfeifer, 2003; Kaneko, Kanayama, & Tsuji, 1998; Solomon & Hartmann, 2006; Wijaya & Russell, 2002) in that the approach taken is based more closely on the anatomy and neurophysiology of the rat whisker sensory system. We have adopted artificial design solutions that endow more biological plausibility than intuitive engineering utility, a philosophy more akin to the "brain-based devices" construct (Seth, McKinstry, Edelman, & Krichmar, 2004).

The next section contains a brief overview of the rat and the morphology of their facial whiskers. This is then compared, in the following section, to the robot implementation that has been built, including an overview of the gross processing and control systems. The next section contains a more detailed overview of the electronic hardware used to implement the neural

models of the various components of the rat brain and how they have been integrated into the robot communication and control architecture. The following two sections contain a combined biological description and engineering interpretation of the "front end" of the whisker sensory system, namely, the follicle sinus complex at the root of each whisker and the primary afferents that innervate them. The neuroethology of rat "whisking" is detailed in the subsequent section, again with a description of how this has been interpreted and implemented in the robot. This is followed by a section that describes the neurology of action selection and how this has been modeled in the neural control architecture of the robot to drive the motors. The last two sections detail the orientation behavior observed in rats in response to vibrissal stimulation and how this has been interpreted on the robot. This is supported by demonstrative experiments of the mobile robot performing active touch and orient to stimulus behaviors in a real-world environment.

2   The Rat

An adult rat (*Rattus norvegicus*) has a nominal length of 400 mm (including tail) and weighs an average of 300 g (left panel of Figure 1). It has in the region of 30 macro-vibrissae on either side of the snout, arranged into five rows of six whiskers protruding from a muscular surface called the mystacial pad, and 60 micro-vibrissae located more rostral-ventrally (see central panel of Figure 1 for description of terminology) as well as in and around the mouth. The length of each macro-vibrissae in a row decreases exponentially the more rostral its location. The curvature of each macro-

vibrissa also depends on its dorso-rostral location in the mystacial pad, more rostral whiskers tend to curve more rostrally. The vibrissae are composed of keratin, similar to hair but much thicker, measuring between 50 and 20 μm at the base tapering to approximately 5 μm at the tip (Haidarliu & Ahissar, 2001).

3   The Robotic Platform

Whiskerbot (right panel of Figure 1) consists of a "head" sensory unit that measures 150 mm by 170 mm, and a "body" which is currently a two-wheeled differential drive platform developed prior to the project for general mobile robotic experimentation. The head sensory unit has been designed to accommodate six whiskers arranged into rows of three on each opposing "cheek" of the unit. To approximate the curvature and tapering of a nominal rat whisker a two part aluminum mold was built to form glass-fiber composite whiskers with a maximum length of 200 mm (four times the length of the largest vibrissae measured on a rat). This approach differs from other similar projects (Kaneko et al., 1998; Solomon & Hartmann, 2006; Wijaya & Russell, 2002), which used artificial whiskers made from spring steel with no curvature or tapering as observed in rat vibrissae. The minimum cross-sectional diameter of these molded whiskers at the base was constrained by the size of the four strain gauges that were bonded to the periphery. The diametrically opposing gauges were electrically connected into two half bridges (wheatstone) generating strong strain measurements in response to deflections in the whisker shaft in two axes of freedom referred to as "*x*" (rostro-caudal plane) and "*y*" (dorso-ventral plane). The use of resis-
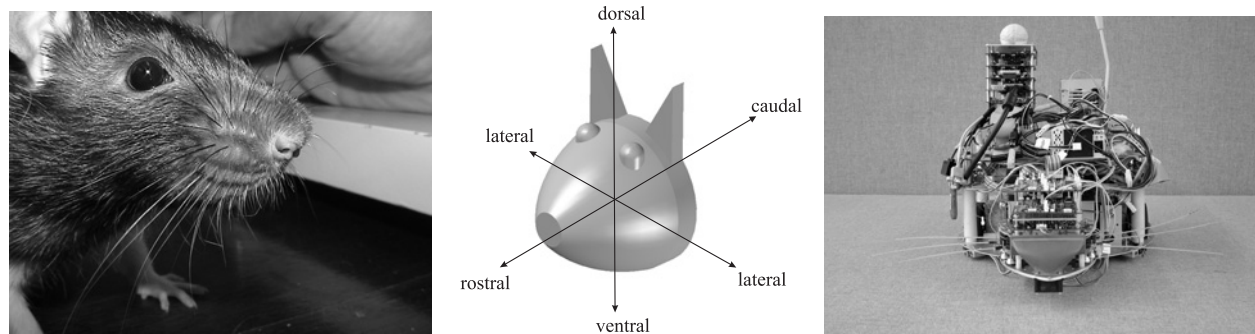

Figure 1   Photographs of the six whisker head sensory unit mounted on the differential drive robot body, (Whiskerbot) and a close up of the head and mystacial vibrissae of a live rat.
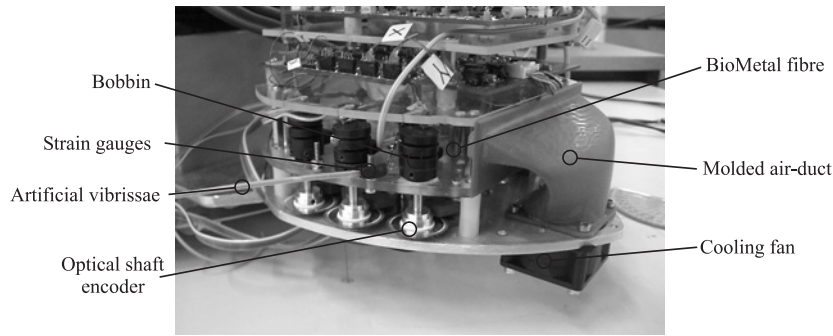
Figure 2   Photograph of the head sensory unit detailing the key components.

tive strain gauges was chosen to derive stable deflection vectors as this is not possible using microphones (Fend et al., 2003).

Each whisker is mounted into a plastic bobbin, which in turn is located onto a shaft held between two plates by low friction bearings (see Figure 2). Optical shaft encoders are also located on these shafts to derive an absolute angle of each whisker with respect to the head unit. Shape metal alloy fiber (BioMetal®) was wrapped around the shaft-mounted bobbins and secured to anchor points 100 mm behind. BioMetal contracts longitudinally when heated, reducing by up to 10% of its original length when heated through 70°C. When a current is passed through the BioMetal fiber the contraction caused by the electrical heating is translated into rotation of the bobbin and a consequential forward sweeping movement of the attached whisker. When the current is removed the fiber begins to cool and the whisker returns to its original resting position, assisted by a small spring attached to the bobbin. To dissipate the heat from the fibers more rapidly a fan has been used to force air across them via a specially molded duct to provide a consistent air flow. This forward, and then backward, sweeping of the whisker shaft is comparable to the whisking behavior observed in rodents and the actuation mechanism chosen to be analogous to the linear contraction of the mystacial intrinsic musculature associated with each vibrissae (detailed in a later section). Again this choice of actuation was principally guided by biological plausibility rather than engineering utility, however, the benefits of using Bio-Metal fiber, as opposed to conventional rotating electric motors, were that it is compact, lightweight and generates very little noise. To control the heating of the BioMetal actuators, pulse width modulated (PWM) sig-

nals are generated by associated micro-controllers (dsPIC30F4011), the duty cycle of the signal being proportional to the current delivered. The same micro-controllers also measure the angle of whisker rotation from the optical shaft encoders using the on-chip quadrature encoder interface. Each micro-controller associated with a whisker is connected via a shared serial peripheral interface (SPI) bus to a single field programmable gate array (FPGA) located on a reconfigurable computing platform (described further in next section). This FPGA sends the desired drive signals to the individual whisker micro-controllers and reads in the current angle of the whiskers every 0.5 ms (2 kHz). This same FPGA also reads in the x and y strain values from each whisker, at 0.1 ms intervals (10 kHz), sampled by a separate DSP micro-controller (Texas Instruments, model TMS370f2812) and connected to the FPGA via another SPI bus. A further SPI bus connects the FPGA to the robot platform controller (dsPIC30F4011). FPGAs were used due to their large and flexible input/output availability and the capacity to perform customized parallel processing for very high computational throughput. This was found to be necessary for updating the models of neural structures, detailed in the next section, in a biologically plausible measure of real-time.

Both the head sensory unit and the robot platform body are powered from a single 13 Ah lead acid battery. To generate the different voltages required by the various components of the system, an ATX power supply and 12 V DC–240 V AC inverter have been temporarily installed on the platform. This allows up to 2 h of experimentation between battery recharges, alternatively the ATX unit can be powered using a 240 V AC supply and trailing extension lead.

4 Neural Modeling Hardware

The computational neuroscience models of whisker sensory processing that we have developed are implemented on a Nallatech BenNuey PC104plus reconfigurable computing platform. This platform contains a conventional single board computer (SBC) with an Intel Celeron processor (650 MHz), 512 Mb of SDRAM (133 MHz FSB), graphics accelerator, 2× USB, ethernet, sound i/o, PS/2 and an associated 40 Gb 2.5″ harddrive. The PCI bus of this SBC is connected to the BenNuey motherboard, physically located above the SBC with the same PC104 outline. The motherboard consists of five layers; the PCI interface card, user FPGA card and three expansion cards into which a family of compatible modules can be installed. The FPGA devices installed on the motherboard for the Whiskerbot project were three Xilinx Virtex-II X2V8000 (8 million equivalent logic gates each), one on the user FPGA card and two on a single BenBlue-II plug-in module installed onto one of the expansion cards. This platform has been used to closely couple software and

hardware models to facilitate real-time performance of detailed, large-scale, embedded sensorimotor neural systems. Figure 3 shows how the BenNuey system has been integrated with the rest of the robot platform, detailing the main communication pathways and processing blocks. The SPI buses, relaying the raw sensory data from the strain gauges bonded to the vibrissae and the whisk angle information from the shaft encoders, are mastered by the user FPGA to maintain the synchronization of data flow and to centrally co-ordinate the multi-processor architecture of the head sensory unit.

The data is passed to concurrently operating processing elements instantiated within the FPGA to maximize computational throughput. A collection of such elements have been constrained into a single component, or core, that has been called the "Mechano-Processor" (Pearson, Gilhespy, Melhuish, et al., 2005). It contains all the elements that are responsible for external communication with the head sensory module and robot platform, and the generation of numerous biologically plausible spike trains representing the
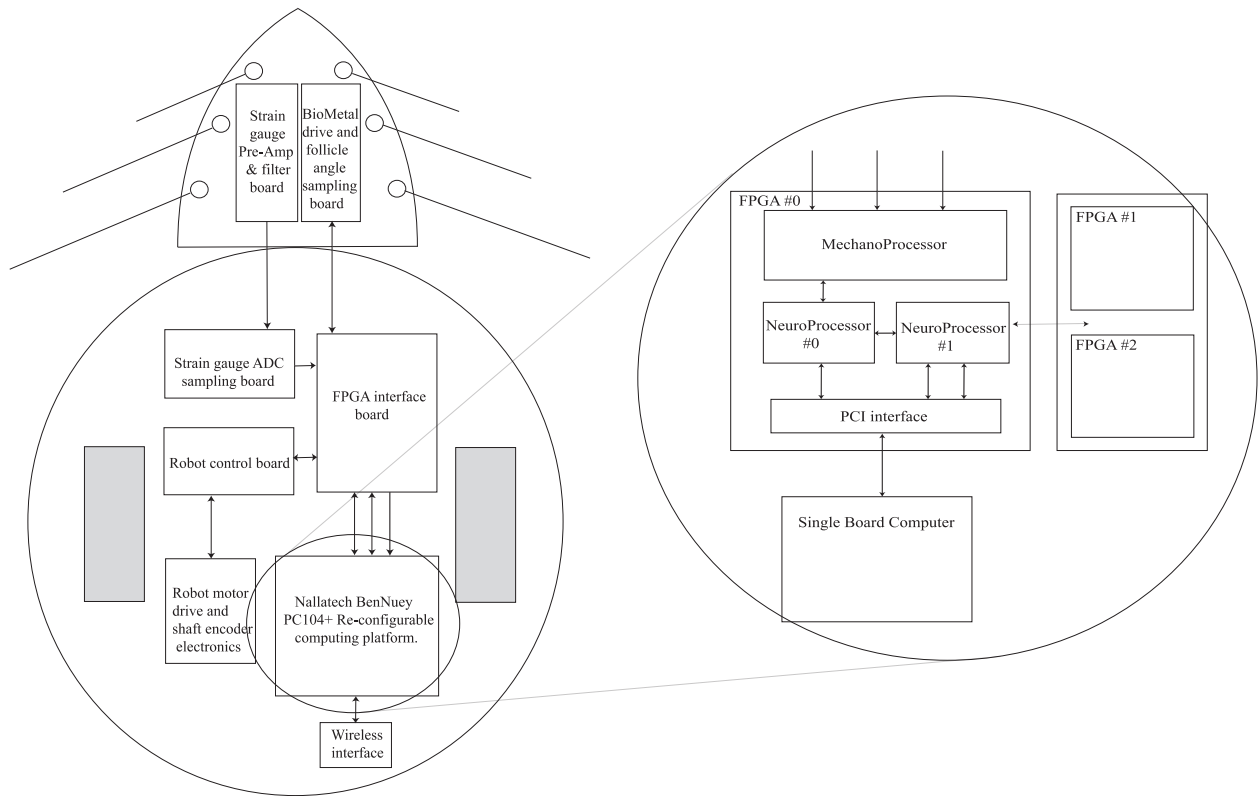

Figure 3 Communications and processing topology of Whiskerbot. Inset: The communications and processing architecture within the BenNuey PCI104+ reconfigurable computing platform.

activity of primary afferents projecting to the brain stem from the vibrissae. The output spike trains from this core are passed into an array of strictly real-time spiking neural network processor cores, or "Neuro-Processors" (Pearson, Gilhespy, Gurney, et al., 2005), which are each capable of updating 640 Leaky-Integrate-and-Fire neuron models and 10240 synapses in 0.5 ms independent of their activity or connectivity. Neuro-Processor cores are cascaded together via their asynchronous I/O modules that pass the current state of each neuron connected to the module as a single bit (1 spiking, 0 not spiking). The inter-core I/O modules can be connected internally for multiple NeuroProcessor cores on the same device as well as externally via the physical pins of the device to build multi-chip arrays. Experiments consisting of eight NeuroProcessors instantiated on the three FPGAs of the current Ben-Nuey platform have been implemented and demonstrated maintaining a real-time, network-wide performance. The I/O modules of the NeuroProcessor cores can also be connected to another specialist FPGA core that interfaces the PCI bus to the SBC. C/C++ API function libraries are supplied from the BenNuey platform vendor that can both send and receive data via the PCI bus to the hardware. These have been used to write a process that interfaces the hardware instantiated neural models in the FPGA with the software implemented models in the SBC. For developmental purposes this also allows access to the raw sensory data from the head module and to monitor the state of the neuron models and other internal states of the hardware.

5 Follicle Sinus Complex Model

The root of each vibrissa is encased within a follicle that is set beneath the skin of the mystacial pad. Figure 4 (taken from Ebara, Kumamoto, Matsuura, Mazurkiewicz, & Rice, 2002) details the anatomy of follicles in a cat and a rat, highlighting the inter-species similarities of this structure. The follicle is composed of numerous membranes and blood-filled sinuses, hence follicle sinus complex (FSC), and contains a large number of mechanoreceptive cells (Ebara et al., 2002). The location of these cells within the structure of the FSC largely determines how they respond to the mechanical deflections that translate along the length of the vibrissal shaft. For example, the receptive cells located in the inner and outer root sheaths (labeled as
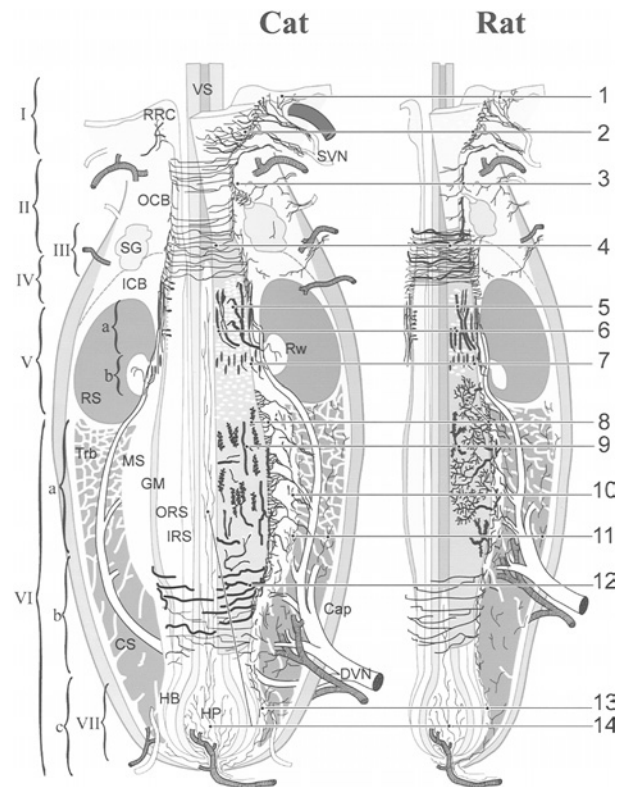

Figure 4 Comparative cross-section of rat and cat follicle (Ebara et al. 2002)© (Reprinted with permission of Wiley-Liss, Inc., a subsidiary of John Wiley and Sons, Inc.).

IRS/ORS on Figure 4) will respond proportionately to the magnitude of deflections of the vibrissa. However, receptive cells within the mesenchymal sheath (MS), which is separated from the root sheath by a stiff layer called the glassy membrane (GM), will tend to respond only to the derivative of deflections of the shaft. In Whiskerbot, this mechanical filtering has been modeled using a mass-spring-damper analog and further abstracted to two fourth order infinite impulse response (IIR) filters implemented in FPGA hardware. The strain vectors derived from the strain gauges at the base of each vibrissa are passed through both filters to provide two sets of input stimuli for the primary afferent models detailed in the next section.

Projecting from each FSC are two nerves containing the axons of the primary afferent (PA) neurons that innervate the mechanoreceptive cells within the FSC. In a rat the superficial vibrissal nerve (SVN, Figure 4) conveys the PAs that innervate the mechanore-

ceptive cells populating the upper sections of the FSC, principally the circumferentially oriented cells around the union of the inner and outer conical body (ICB/OCB). These cells and their subsequent excitation of the PAs that innervate them, have been postulated as responsible for encoding the angle of the FSC with respect to the skin of the mystacial pad during active whisking (Szwed, Bagdasarian, & Ahissar, 2003). The deep vibrissal nerve (DVN) conveys the PAs that innervate the lower regions of the FSC, which are isolated from movements of the follicle itself, instead encoding only "touch"-specific information as the vibrissa shaft is deflected. In Whiskerbot, the strain gauge information can be interpreted as being via the DVN, and the follicle angle (with respect to the rostro-caudal axis of the robot derived from the optical shaft encoders) as via the SVN.

6 Primary Afferents Model

There are approximately 200 PAs projecting from each FSC to the trigeminal sensory cortex (brain stem) of a rat. As a result of the non-homogeneous distribution of mechanoreceptive cells which the PAs innervate in the FSC, each PA has different response characteristics to deflections of the vibrissal shaft. The rate at which the PA average spike activity adapts to a step deflection has been used to coarsely classify them

into slowly adapting, with adaptation time constants in excess of 100 ms, and rapidly adapting, characterized by shorter time constants. It has been postulated that the rapidly adapting PAs tend to innervate the mechanoreceptors located within the mesenchymal sheath layer of the FSC whereas the slowly adapting PAs innervate those located in the root sheath, as described in the previous section (Mitchinson et al., 2004). Therefore, the physical distribution of the mechanoreceptors and the mechanical characteristics of the FSC actually constitute the initial stage of sensory signal processing. The PAs are further differentiated by their directional sensitivity to vibrissal deflections and the angle of deflection to which they are most responsive (most effective angle). Rapidly adapting PAs also tend to have a non-linear activity relationship to input stimulus in comparison with a more linear response from slowly adapting PAs. All these features have been incorporated into a parameterized PA model, shown in Figure 5, and described more fully in Mitchinson et al. (2004).

In Whiskerbot, this PA model has been implemented in FPGA hardware as a further component within the MechanoProcessor core mentioned earlier. A total of 240 individually parameterized PA models needed to be updated in $100\,\mu s$ (10 kHz), which was found to be appropriate to maintain an acceptable level of model integrity. To achieve this computational throughput, the hardware was configured into a pipe-
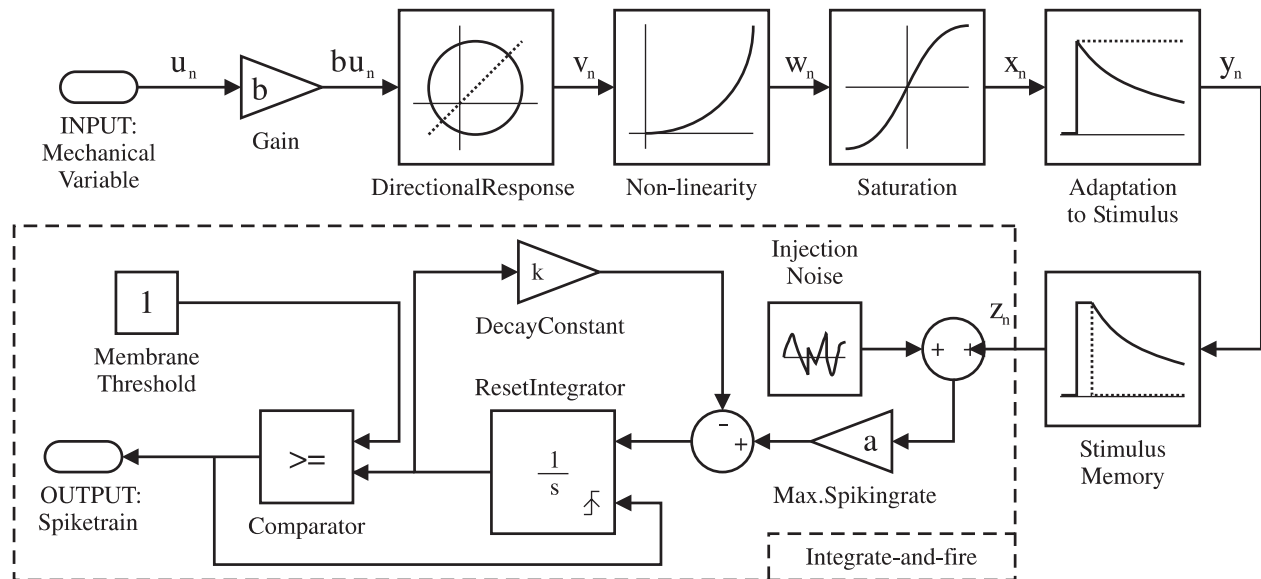

Figure 5 Primary afferent model. Taken from Mitchinson et al. (2004).
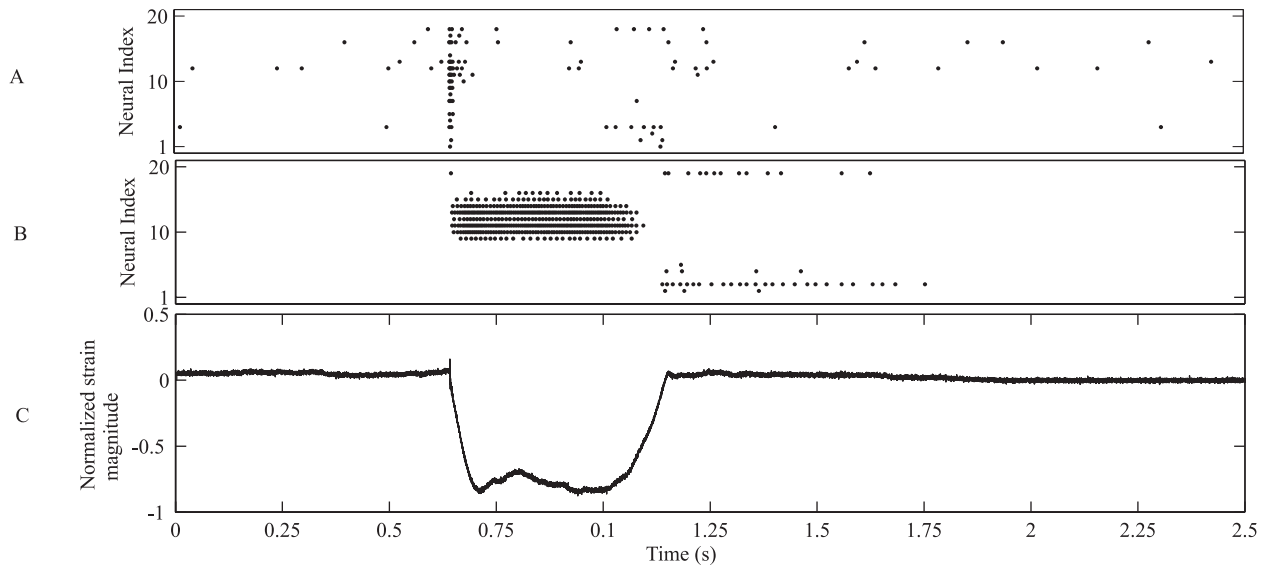
Figure 6 (A) Rapidly adapting primary afferent spike response to deflection of artificial vibrissal shaft. (B) Slowly adapting primary afferent spike response to same deflection. Most effective angle (MEA) of each PA (both rapidly and slowly adapting species) is uniformly distributed around vibrissae shaft, 0 radians set as neuron 0 therefore neural index 10 having an MEA of π radians. (C) Normalized *x*-strain magnitude measured in vibrissal shaft.

line, each feature of the PA model shown in Figure 5 forming a separate stage or processing element. Each processing element contains the necessary hardware to perform the specific task, which may include multipliers, adders and local contextual memory. This allows each element to operate concurrently, requiring synchronization between adjoining elements in the pipeline only when an input is required or an output has been generated. After each element in the pipeline has been loaded, the system updates an entire PA model in the time taken by the slowest element in the chain to perform its operation, which is approximately 13 rising clock edges. Using a clock of 40 MHz means that all 240 PA models are updated in 80 μs, a computational performance approximately equivalent to a 500 MHz conventional digital signal processor (DSP). An example spike output from the PAs of a single FSC model in response to a static deflection of the vibrissae is shown in Figure 6. The vibrissa was clamped at the base and displaced caudally at the tip by approximately 30 mm, held for a short period of time (approximately 0.5 s), and then released. The normalized magnitude of the *x*-plane strain gauges is displayed in the lower panel with the resultant spike output from the 40 PA models of the FSC in upper two panels. The 20 rapidly adapting PAs (top panel of Figure 6) respond strongly to the deflec-

tion onset but then rapidly attenuate, whereas the 20 slowly adapting PAs (middle panel) maintain their activity for the duration of the deflection. The directional sensitivity of the slowly adapting PAs compared to the rapidly adapting is also clearly visible. This matches empirical data taken from electrophysiological studies of the vibrissal PAs of rodents. Given that the most effective angle (MEA) of each PA has been uniformly distributed around the vibrissal shaft, the direction of the deflection is discernable. This ability could be useful to determine object orientation as the whiskers are swept across an inclined surface.

7 Control of Artificial Whisking

The musculature of the rat mystacial pad consists of intrinsic muscles that are associated with each vibrissa, and extrinsic muscles that are associated with each mystacial pad of the animal (one on either side of the face). An intrinsic muscle protracts an individual vibrissa by pivoting the follicle around the union with the cutaneous plate into which it is anchored. The extrinsic muscles actively retract all the vibrissae on each mystacial pad by pulling the skin backwards, thus pivoting the follicle around the aperture in the mystacial skin.
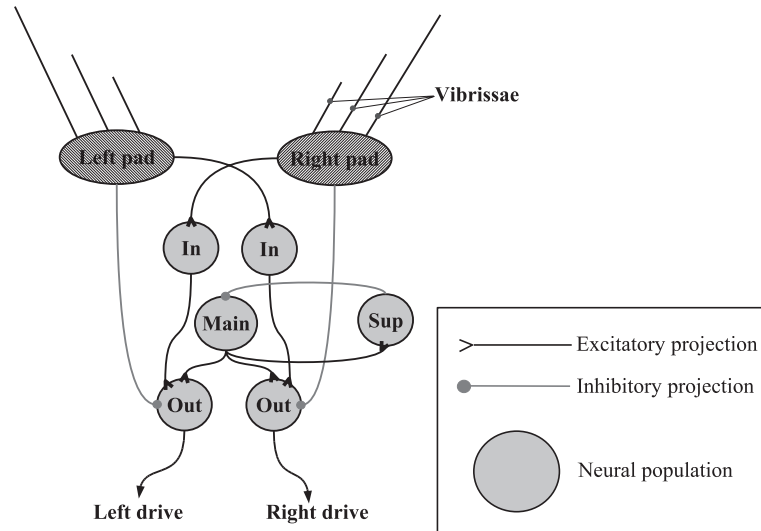
Figure 7 Population diagram of the whisker pattern generator implemented in FPGA hardware. Populations labeled "In" receive excitatory stimulus from the slowly adapting PAs of the contralateral mystacial pads ("left pad"/"right pad"). In turn these nuclei excite the corresponding "Out" nuclei, thus strengthening the resultant whisk drive force to the contralateral vibrissae (maximal contact). The slowly adapting PAs from each pad also directly inhibit the ipsilateral "Out" nuclei, thus attenuating the whisk drive throughout duration of contact (Minimal impingement). The spontaneous current of the neurons that constitute the "Main" nucleus and the inhibitory strength and membrane time constant of neurons that constitute the "Sup" nucleus set the global period of the whisk rate.

The whisk pattern and phase of vibrissae on both mystacial pads are closely coupled, however, this coupling is much stronger between vibrissae on the ipsilateral pad compared to their contralateral counterparts. During "free-whisking", that is, when none of the vibrissae make external contact, the coupling between whisk patterns of vibrissae on contralateral pads is strong. However, the asymmetry between the whisk phases becomes more pronounced when an object is encountered by vibrissae on one side of the head. It has been conjectured that this behavior is the result of two coupled central pattern generators, located somewhere in the brain stem of the rat, that directly regulate the neural motor signals to the muscles on either side of the face (Berg & Kleinfeld, 2003; Nguyen & Kleinfeld, 2005). This conjecture is further supported by ethological observations of unilateral whisking, contact-mediated bilateral adaptation of the whisk pattern (Sachdev, Berg, Champney, Kleinfeld, & Ebner, 2003) and the anatomical fact that the intrinsic muscles are devoid of proprioceptive nerve endings (Rice, Fundin, Pfaller, & Arvidsson, 1994), suggesting a non-conventional positional feedback control mechanism.

In the Whiskerbot project, a spiking neural network was used to reproduce these ethological observa-

tions using the conjectured coupled central pattern generator. Six populations of 24 spiking neurons were used to build a coupled pair of pattern generators to drive the vibrissae located on the two artificial mystacial pads (see Figure 7). To this network, which is referred to as the whisker pattern generator (WPG), were added inhibitory projections from the slowly adapting primary afferent models from vibrissae on the ipsilateral mystacial pad and excitatory projections from those on the contralateral pad. Therefore, when contact is made by the vibrissae on either side, there is a reduction in the drive force to vibrissae on the same mystacial pad and an increase in those of the opposing set for the duration of the deflection. If the object is removed from the vibrissal whisk arc to prevent further contact, the whisk pattern returns to a balanced state. This phenomenon has been called minimal-impingement, maximal-contact (Mitchinson et al., 2006) and could be employed to improve the performance of the sensory system by maintaining clean, stereotypical contacts ipsilaterally to the object while increasing the chance of further contacts by the contralateral vibrissae.

This network was implemented using leaky-integrate-and-fire neuron models updated in real-time using an FPGA instantiated NeuroProcessor core. The actual
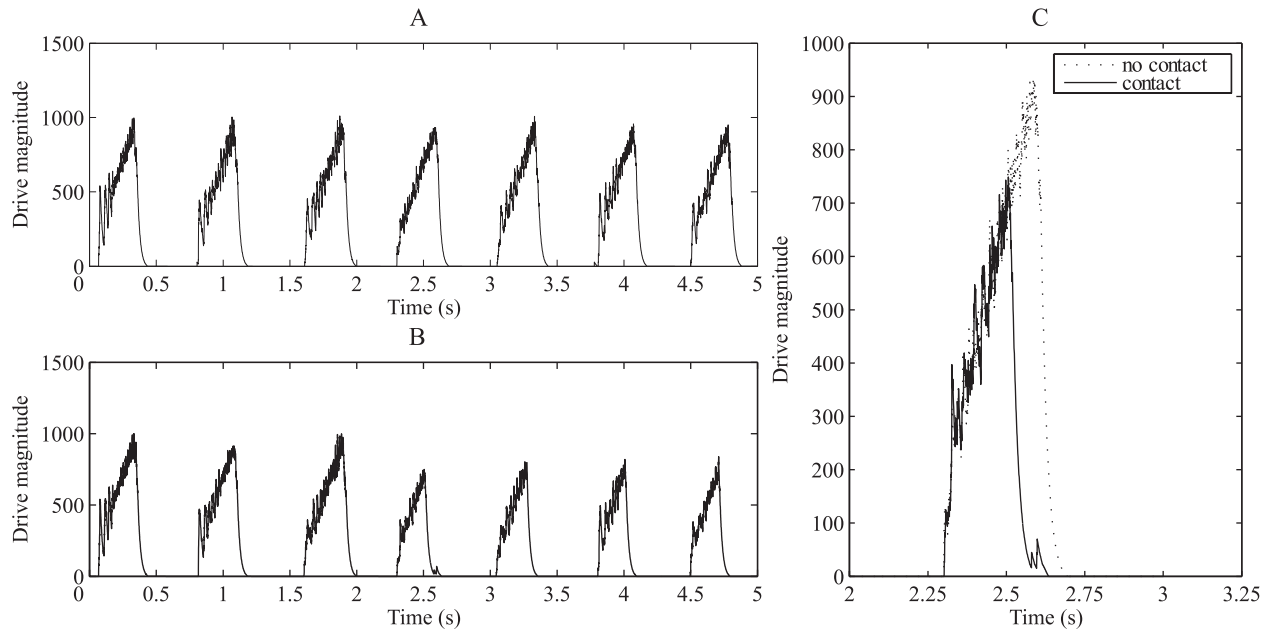
Figure 8   Typical drive signals derived from the whisker pattern generator during 5 s runs. (A) Free-whisking; (B) Contact with an object mid way through the fourth whisk protraction phase; (C) Detailed comparison of fourth whisk taken from plots A and B.

drive signal was derived from this network by integrating the spike response of the neurons in each output population, that is, a population activity representation. This was then scaled and passed directly to the follicle drive micro-controllers to set the duty cycle of the PWM that heats the BioMetal actuators. An example of a typical drive-signal-derived from this Whisker Pattern Generator during a 5 s experiment of free-whisking (no contact) is shown in the top left panel of Figure 8. The lower left panel of this figure shows the influence that the vibrissa making contact with an object has on the drive signal. An object was moved into the whisking arc on the fourth cycle and remained for the duration of the 5 s run. The right hand panel contains a more focused comparison of the signals generated during the fourth whisk cycle highlighting the strong attenuation of the drive signal at the point of contact.

8   Control of Robot Motors

Situated within a sensory rich environment, the number of possible actions that an animal could undertake at any one time is potentially very large. Hunger, fear and other motivations also generate a large number of possible actions or behaviors that an animal may exhibit.

Many of these actions will be complementary to each other and would be impossible to combine into a single hybrid action. To resolve this conflict, an area of the brain called the basal ganglia has been proposed as the centre for action selection (Prescott, Redgrave, & Gurney, 1999; Redgrave, Prescott, & Gurney, 1999). Each of the possible actions or behaviors can be associated with a degree of salience relative to each other that rises and falls depending on external sensory and internal motivational states. The action with the highest salience at any one time could therefore be classed as the "winning" action that should be enacted by enabling control of the relevant muscle groups. This arbitration by the basal ganglia essentially selects the winning action by dis-inhibiting the necessary motor projections while strongly inhibiting those desired by other actions. Switching between actions is smoothed by a degree of hysteresis, and it has been conjectured that this is derived from thalamo-cortical projections, although we have so far modeled this at a more abstract phenomenological level.

In Whiskerbot there are currently three possible actions that can be performed at any one time; "orient to stimulus", "explore environment" or "dead reckoning" (see Figure 9). Dead reckoning is a hard-wired behavior that is not based on any ethological analogue, instead
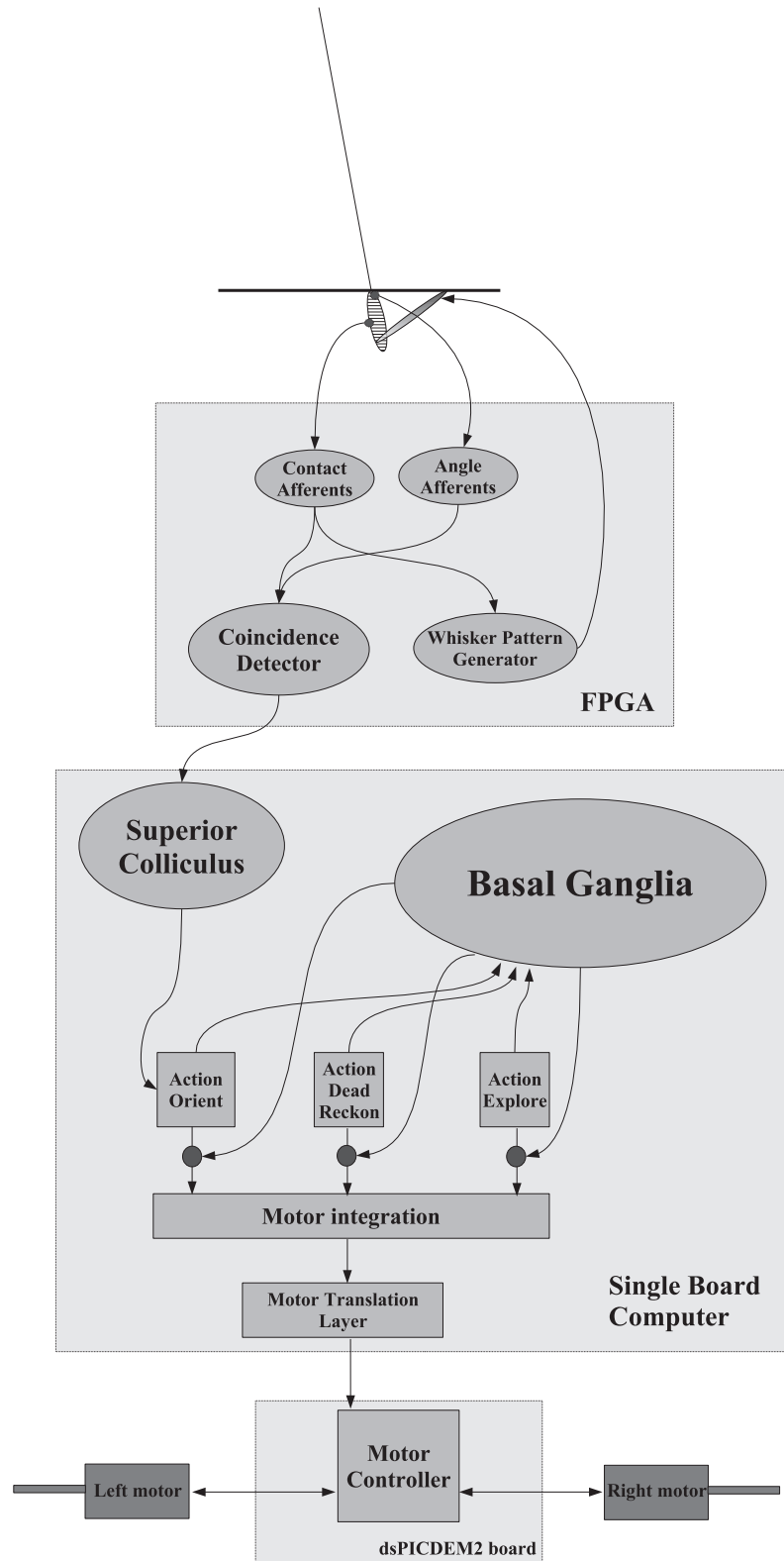
Figure 9 Summary of processing and data flow diagram of current Whiskerbot neural control architecture, highlighting the underlying processing modality of each component. Elliptical-shaped components represent biologically inspired neural models while rectangular blocks indicate where more abstract engineering solutions have been employed.

using conventional path integration to navigate the robot to a desired position. This behavior was added to demonstrate that the neural-inspired architecture can be used to integrate conventional as well as biologically plausible robotic sensorimotor control paradigms. Explore environment is another hard-wired behavior that drives the wheels of the robot to generate a slow sinusoidal searching pattern forwards across the floor, loosely based on an idealized rat exploratory strategy. Orient to stimulus is a behavior that models the observed orient response of rats towards contacts made by their vibrissae. All three of these actions are represented as channels through a model of the basal ganglia, based on the publication by Prescott, Montes Gonzalez, Gurney, Humphries, and Redgrave (2006), and are each associated with a salience. The action with the highest salience is dis-inhibited from relaying its desired motor commands onward. The dis-inhibited motor commands are sent to a software module called the motor translation layer, which generates drive signals for the actuators of the target robotic platform. These signals are then distributed, via the SPI bus, to the motor control board of the robot. The motor control board has a dsPIC micro-controller to implement a local proportional derivative (PD) feedback controller for each of the two motors of the robot platform. The drive signals it receives from the motor translation layer module are converted into duty periods for the PWM signals that energize the motors. The controller has a 50 Hz update rate with a default to 0% duty period and a watchdog timer for fail-safe. The parameters of the PD controller in the dsPIC can be set via the same SPI bus that sends the desired drive signals. This was added to remove the necessity of reprogramming the controller if re-tuning was required. For reference, the progress of the wheels as they are turned by each motor is passed back from the dsPIC to the FPGA via the SPI bus and is used by the dead reckoning action for path integration.

9   Orient to Stimulus

The salience of the orient to stimulus action is derived from the activity of a neural network model of the superior colliculus. This is a neural structure within the mid-brain which is used to conflate multiple sources of sensory input into a head-centric mapping of interesting stimuli in an animal's immediate environment. It consists of multiple layers of neurons with receptive fields consistent with a topographic representation of a particular modal sensori-centric view of the environment, that is, visual field, vibrissae, auditory and so forth. Neurons within the sensory input layers have strong excitatory local projections and inhibitory projections to more distal neurons. The result is a winner-takes-all mechanism whereby the strongest regions of activity tend to rapidly become the most prominent across the neural surface. There are projections to the superior colliculus from a nucleus located in the trigeminal sensory complex of the brain stem called interpolaris (Jacquin, Barcia, & Rhoades, 1989). In turn there are projections to this nucleus from the rapidly adapting primary afferents of the FSCs of the vibrissal array, via the deep vibrissal nerve, and the whisk angle sensitive afferents projecting via the superficial vibrissal nerve (Arvidsson & Rice, 1991). Together these inputs have been used to build a proposed "coincidence detector"[1] that generates a vibrisso-centric representation of angle of contacts made during the protraction whisk phase (Mitchinson et al., 2006). This information, combined with a fixed morphological and topological knowledge of the vibrissae in the mystacial pad, could be used to generate the head centric representation of contact in the superior colliculus. A desired position for the "fovea" (in this case the front tip of the head of the robot) to move to the point of contact is derived from this map and is accompanied by a proportional increase in the salience through the basal ganglia channel for the orientation action. If the basal ganglia selects this action then the orientation motor requests from the orient action are dis-inhibited and consequently released to the motor translation module of the robot. An example of a typical orient to stimulus action response of the robot upon detecting an object using the artificial vibrissae is detailed in the next section.

10   Experimental Results: Orient to Stimulus

The robot was placed into the test arena and 30-s runs were initiated remotely via a USB Wireless LAN interface and the remote desktop facility of Windows XP operating system. The whisk rate was configured to approximately 1 Hz and the gains of the slowly adapting and rapidly adapting primary afferent models
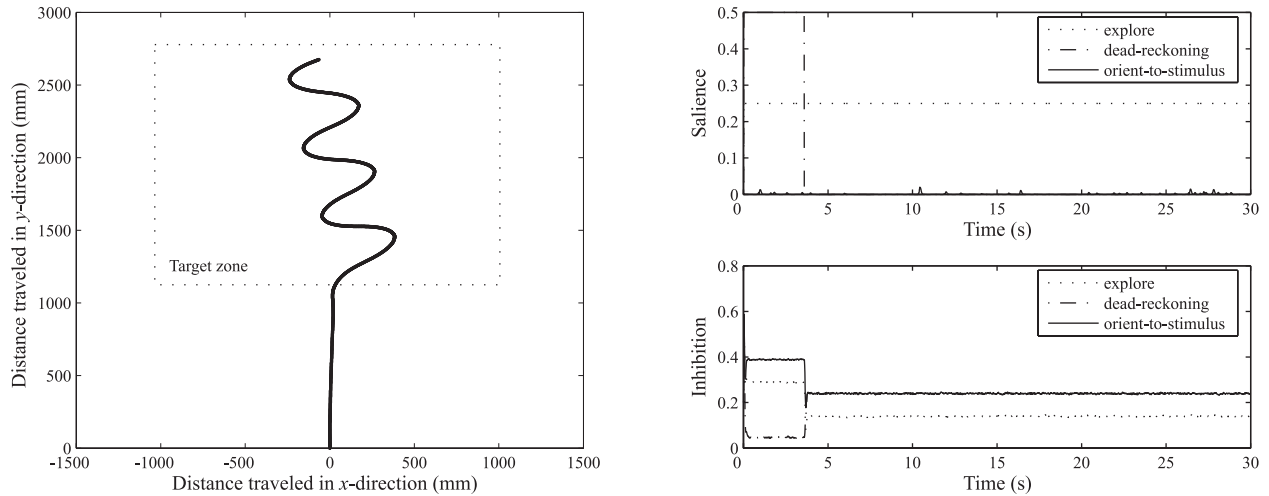
Figure 10 Plots of data taken during a typical 30-s run of Whiskerbot. Left panel shows progress of robot as it moves across the floor, taken from monitoring the rotation of each wheel. Right top panel shows the salience from each behavior throughout the run with the lower panel detailing the resultant level of inhibition projecting back from the basal ganglia to each behavior.

set to reduce spurious orientations triggered by noise. The dead reckoning action was set to have the highest salience at the beginning of a run to locate the robot into the target zone of the arena. The salience to continue this action would decline rapidly when the robot arrives in the target zone resulting in an action switch in the basal ganglia to the explore behavior. The salience for this action is constant and can be considered as the default behavior of the robot. The sweeping motion of the robot provides a much greater chance of vibrissal contact within the target zone and coarsely approximates to an idealized rodent exploratory behavior. The first run highlights the path taken by the robot without finding any objects in the target zone. Figure 10 shows a trace of the robot's movement across the floor in the left panel, with the right panels detailing the salience of each behavior (top), and the consequent degree of inhibition to each from the basal ganglia (bottom). The pre-programmed fall in salience of the dead reckoning behavior from 0.5 to 0 when the target zone is reached, and the subsequent switch to the explore behavior, is clearly visible approximately 4 s into the run and corresponds with the change in robot motion from straight ahead to the exploratory sinusoidal sweeping pattern.

Figure 11 shows the same data set taken from another 30-s run, in which a contact is made with an object in the target zone. When a vibrissa makes contact with the object, in this case a pen balanced on its end, the salience to orient to this stimulus increases sharply in response to the corresponding rise in activity within the superior colliculus. When this sufficiently exceeds the salience of the explore action, the basal ganglia inhibits explore and dis-inhibits the orient to stimulus action. The robot then enacts appropriate motor movements to bring the nose of the sensory head module to the source of contact. After a set period of time the robot reverses away from the source of contact (points 2 to point 3) and returns to the default explore behavior as can be seen in the salience and inhibition plots of Figure 11. Figure 12 shows photos of the experimental set up (left panel), the robot during the explore behavior (top right) and during an orient to stimulus action (bottom right).

The rapidly adapting PA spike response and whisk phase angle from the two front whiskers during this run are displayed in the top two panels of Figure 13. Each point on the PA plots indicates that a particular neuron (indexed 0–20) generated a spike at that time. The bottom panel contains the spike response from the coincidence detector, the dotted line indicating the boundary between neurons sensitive to the front left (neural indices 0–23) and front right (neural indices 24–47) whiskers. The contact point is clearly identified by a sharp rise in the spike activity of the contact PAs of the front left whisker and the disturbance in the
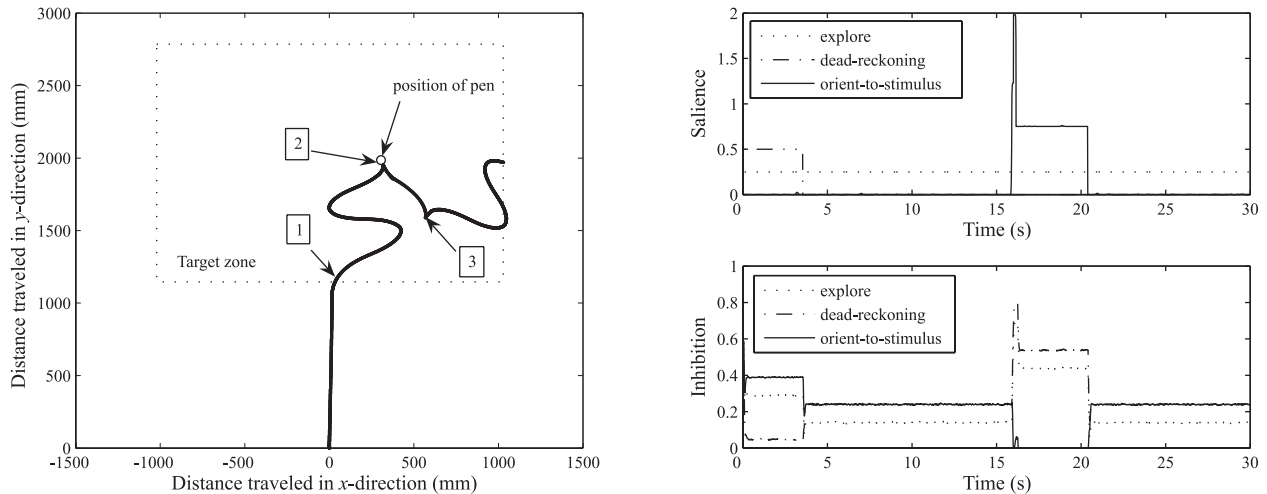
Figure 11   Same format of data as in Figure 10 taken during another 30-s run of Whiskerbot: (1) Robot reaches target zone using the dead-reckoning behavior at which point it switches to explore. (2) Contact is made by one of the vibrissae with a pen and an orientation response is enacted. (3) After orientation and fixed reverse maneuver the robot continues to explore.
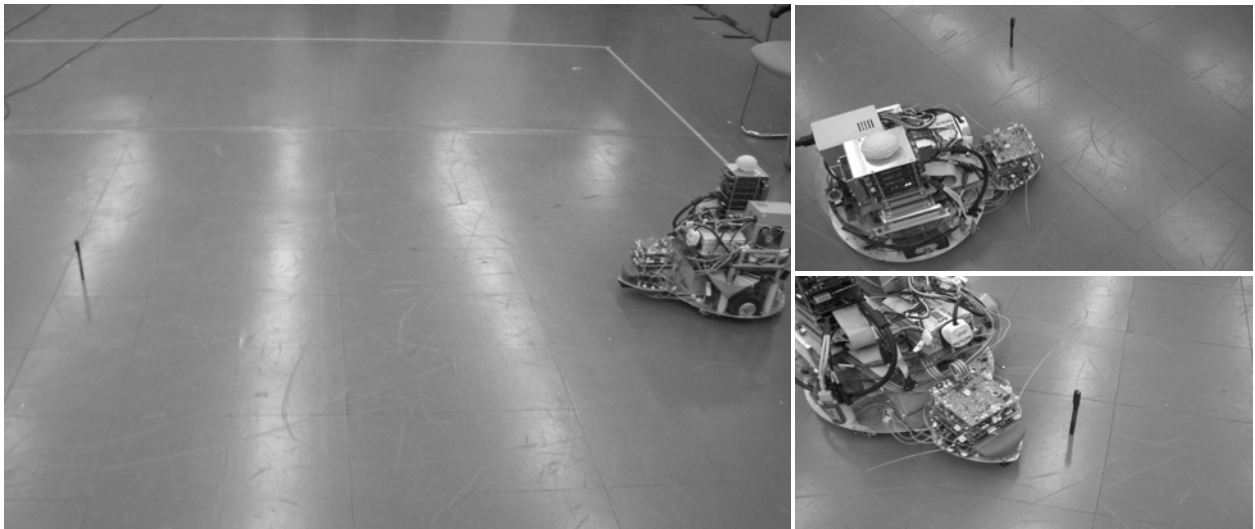

Figure 12   Photographs of the initial experimental set-up and taken during the run in which a pen was located using the left front vibrissae.

regular whisk pattern approximately 16 s into the run. The coincidence between contact and the current whisk angle is represented in the coincidence detector by an increase in spike activity from the corresponding neurons that encode whisk angle. It is this information that is passed to the superior colliculus and ultimately initiates a directed orientation to stimulus behavior.

11 Discussion and Future Work

A biologically inspired robotic implementation of the rat whisker sensory system has been built. This has been used to embody neural control algorithms to reproduce behaviors observed in live rats. Specifically, the phenomenon of contact-mediated adaptation of the whisking pattern displayed by rats, active touch,
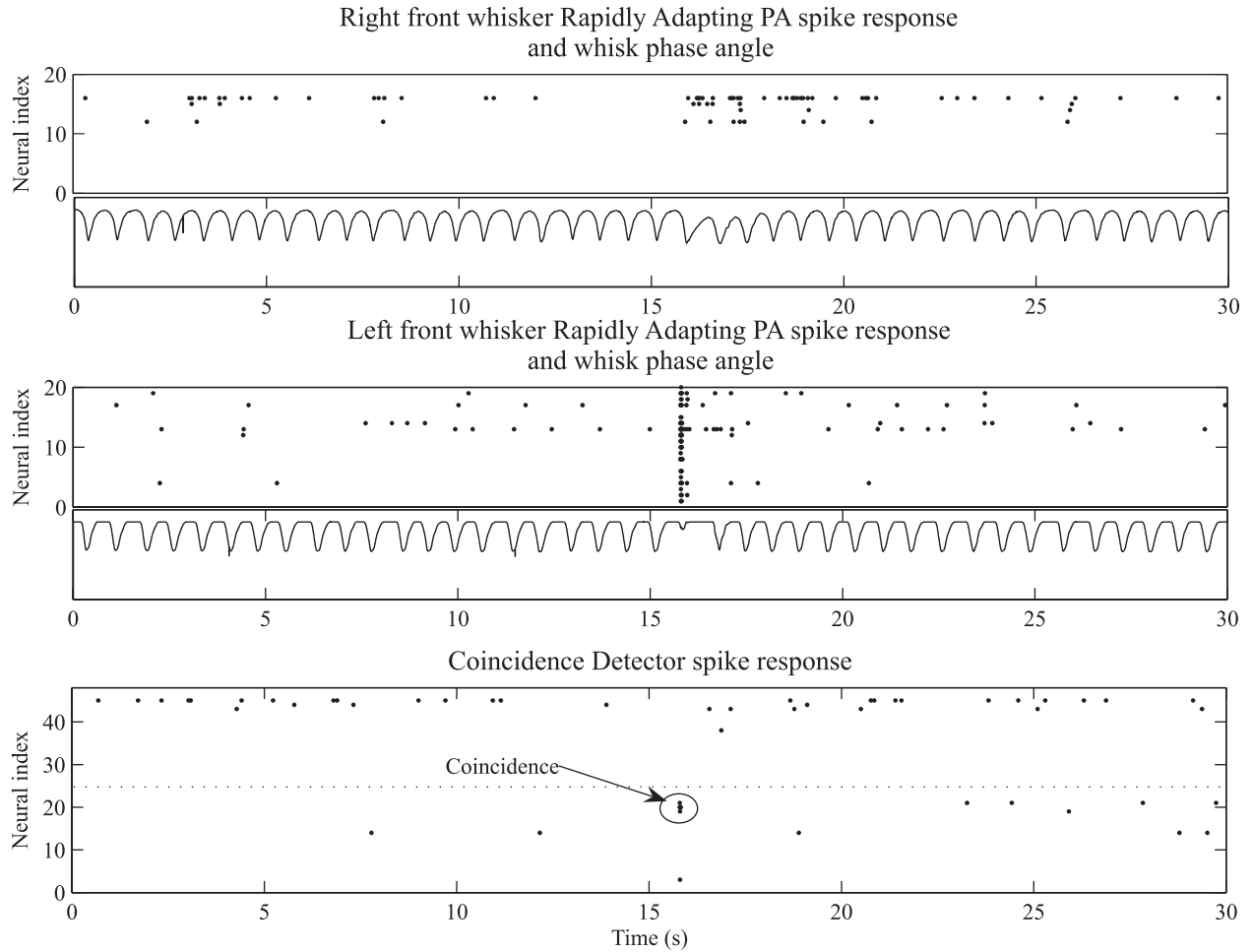
Figure 13 Rapidly adapting PA spike response and whisk angle of front right and front left whiskers from run detailed in previous two figures. Lower panel is the spike response from the coincidence detector taking input from the contact PAs and whisk angle sensitive afferents. Neural indices 0 to 23 of the coincidence detector encode whisk angle of front left whisker and 24 to 47 the front right whisker.

has been physically demonstrated. Furthermore, the sensory information derived from the artificial vibrissae has been used to enact a neuroethologically plausible orientation behavior of the robot. This involved the integration of neural models of superior colliculus, basal ganglia and trigeminal sensory complex at different levels of neural modeling abstraction. The real-time performance of these neural models was achieved by utilizing both hardware (FPGA) and software-based processing constructs

Integrating biologically plausible models of neural structures with a novel tactile sensory system, again based closely on the biological analogy, to demonstrate how adaptive behaviors are mediated in nature provides a useful basis for further investigation. Clearly the orienting behavior demonstrated in this article could have been phenomenologically reproduced using much simpler engineering techniques; however, by attempting to use the mechanisms employed by the brain we can start to investigate how such systems are capable of coordinating more complex behaviors in animals. Our future work plans include the further investigation of the whisker sensory apparatus to determine how this modality contributes towards an animal's spatial cognition. We also plan to integrate the established brain-based behavioral mediation mechanism detailed in this article with further neural models of the rat brain, including hippocampus for episodic

memory and map building, and the amygdala for exploring the role of emotion in sensory conditioning and perception. The use of whiskers for general robotic deployment is also of significant interest, most notably as a robust alternative to vision-based exploration on submarine robots, extra-terrestrial planetary rovers or for medical intracorporeal inspection.

Acknowledgment

Note

1   There is no direct evidence that this transform is performed; rather, it is inferred from the nature of peripheral signals and the assumption that central vibrissal representations are likely to fall into register with those of the other senses in the superior colliculus.

References

Ahl, A. (1986). The role of vibrissae in behaviour: a status review. *Veterinary Research Communications*, *10*(4), 245–268.

Arvidsson, J., & Rice, F. (1991). Central projections of primary somatosensory neurons innervating different parts of the vibrissal skin on the mystacial pad of the rat. *Journal of Comparative Neurology*, *309*, 1–16.

Benedetti, F. (1995). Orienting behaviour and superior colliculus sensory representation in mice with the vibrissae bent into contralateral hemisphere. *European Journal of Neurosceince*, *7*, 1512–1519.

Berg, R. W., & Kleinfeld, D. (2003). Rythmic whisking by rat: retraction as well as protraction of the vibrissae is under active muscular control. *Journal of Neurophysiology*, *89*, 104–117.

Carvell, G., & Simons, D. (1990). Biometric analyses of vibrissale tactile discrimination in the rat. *Journal of Neuroscience*, *10*, 2638–2648.

Dean, P., Redgrave, P., & Westby, G. (1989). Event or emergency? Two response systems in the mammalian superior colliculus. *Trends in Neuroscience*, *12*(4), 137–147.

Di Scala, G., Schmitt, P., & Karli, P. (1983). Unilateral injection of GABA agonists in the superior colliculus: Assymmetry to tactile stimulation. *Pharmacology, Biochemistry and Behavior*, *19*, 281–285.

Ebara, S., Kumamoto, K., Matsuura, T., Mazurkiewicz, J., & Rice, F. (2002). Similarities and differences in the innervation of mystacial vibrissal follicle-sinus complexes in the rat and cat: a confocal microscopic study. *Journal of Comparative Neurology*, *449*, 103–119.

Fend, M., Bovet, S., Yokoi, H., & Pfeifer, R. (2003). An active artificial whisker array for texture discrimination. In *Proceedings of the IEEE/RSJ International Conference on Intelligent Robots and Systems (IROS)* (pp. 1044–1049).

Gurney, K., Prescott, T., & Redgrave, P. (2001). A computational model of action selection in the basal ganglia I: A new functional anatomy. *Biological Cybernetics*, *84*, 401–410.

Gustafson, J., & Felbain-Keramidas, S. (1977). Behavioural and neural approaches to the function of the mystacial vibrissae. *Psychological Bulletin*, *84*, 477–488.

Haidarliu, S., & Ahissar, E. (2001). Size gradients of barreloids in the rat thalamus. *Journal of Comparative Neurology*, *429*, 372–387.

Hartmann, M. (2001). Active sensing capabilities of the rat whisker system. *Autonomous Robots*, *11*, 249–254.

Jacquin, M., Barcia, M., & Rhoades, R. (1989). Structure function relationships in rat brain stem subnucleus interpolaris (VI): Projection neurons. *Journal of Comparative Neurology*, *282*, 45–62.

Kaneko, M., Kanayama, N., & Tsuji, T. (1998). Active antenna for contact sensing. *IEEE Transactions on Robotics and Automation*, *14*, 278–291.

Killackey, H., & Erzurumula, R. (2004). Trigeminal projections to the superior colliculus of the rat. *Journal of Comparative Neurology*, *201*, 221–242.

Krupa, D., Matell, M., Brisben, A., Oliveira, L., & Nicolelis, M. (2001). Behavioural properties of the trigeminal somatosensory system in rats performing whisker-dependent tactile discriminations. *Journal of Neuroscience*, *21*, 5752–5763.

Ma, P. (1991). The barrelettes-architectonic vibrissal representations in the brainstem trigeminal complex of the mouse; a normal structural organization. *Journal of Comparative Neurology*, *309*, 161–199.

Milani, H., Steiner, H., & Huston, J. (1989). Analysis of recovery from behavioural asymmetries induced by unilateral removal of vibrissae in the rat. *Behavioural Neuroscience*, *103*, 1067–1074

Mitchinson, B., Gurney, K., Redgrave, P., Melhuish, C., Pipe, A., Pearson, M., et al. (2004). Empirically inspired simulated electro-mechanical model of the rat mystacial follicle-sinus complex. *Proceedings of Royal Society London (B) Biological Science*, *271*, 2509–2516.

Mitchinson, B., Pearson, M., Melhuish, C., & Prescott, T. (2006). A model of sensorimotor coordination in the rat whisker system. In S. Nol (Ed.) *Animals to Animats 9: Proceedings of the Ninth International Conference on Simulation of Adaptive Behaviour 4095* (pp. 77–88). Springer-Verlag.

Nguyen, Q., & Kleinfeld, D. (2005). Positive feedback in a brainstem tactile sensorimotor loop. *Neuron*, *45*, 447–457.

Pearson, M., Gilhespy, I., Gurney, K., Melhuish, C., Mitchinson, B., Nibouche, M., et al. (2005). A real-time, FPGA based, biologically plausible neural network processor. In *Articial neural networks: Formal models and their applications* (Vol. 3697, pp. 1021–1026).

Pearson, M., Gilhespy, I., Melhuish, C., Mitchinson, B., Nibouche, M., Pipe, A., et al. (2005). A biomimetic haptic sensor. *International Journal of Advanced Robotic Systems*, *2*, 335–343.

Prescott, T., Montes Gonzalez, F., Gurney, K., Humphries, M., & Redgrave, P. (2006). A robot model of the basal ganglia: behaviour and intrinsic processing. *Neural Networks*, *19*, 31–61.

Prescott, T., Redgrave, P., & Gurney, K. (1999). Layered control architectures in robots and vertebrates. *Adaptive Behavior*, *7*, 99–127.

Redgrave, P., Prescott, T., & Gurney, K. (1999). The basal ganglia: A vertebrate solution to the selection problem? *Neuroscience*, *89*(4).

Rice, F., Fundin, B., Pfaller, K., & Arvidsson, J. (1994). The innervation of the mystacial pad in adult rat studied by anterograde transport of HRP conjugates. *Experimental Brain Research*, *99*, 233–246.

Sachdev, R., Berg, R., Champney, G., Kleinfeld, D., & Ebner, F. (2003). Unilateral vibrissa contact: Changes in amplitude but not timing of rythmic whisking. *Somatosensory and Motor Research*, *20*, 163–169.

Seth, A., McKinstry, J., Edelman, G., & Krichmar, J. (2004). Active sensing of visual and tactile stimuli by brain-based devices. *International Journal of Robotics and Automation*, *19*(4).

Solomon, J., & Hartmann, M. (2006). Robotic whiskers used to sense features. *Nature*, *443*(5), 525.

Szwed, M., Bagdasarian, K., & Ahissar, E. (2003). Encoding of vibrissal active touch. *Neuron*, *40*, 621–630.

Van der Loos, H. (1976). Barreloids in mouse somatosensory thalamus. *Neuroscience Letters*, *2*, 1–6.

Vincent, S. (1912). The function of the vibrissae in the behaviour in the white rat. *Behavioural Monographs*, *1*, 1–82.

Welker, W. (1964). Analysis of sniffing of the albino rat. *Behaviour*, *22*, 223–244.

Wijaya, J., & Russell, R. (2002). Object exploration using whisker sensors. In *Proceedings of the 2002 Australasian Conference on Robotics and Automation* (pp. 180–185).

Woolsey, T., & Van der Loos, H. (1970, January). The structural organization of layer IV in the somatosensory region (SI) of mouse cerebral cortex. The description of a cortical field composed of discrete cytoarchitectonic units. *Brain Research*, *17*, 205–242.

About the Authors

Martin J. Pearson received a BEng (Hons) degree in electrical and electronic engineering from the University of Manchester in 1996 and an MSc in advanced technologies in electronics from the University of the West of England, Bristol, UK in 2002. He is currently in the final stages of his PhD degree and is employed as a research associate at the Bristol Robotics Laboratory working on a bio-inspired robotics project. His research interests include real-time FPGA implementations of neural systems, embedded digital signal processing, robotics and biologically inspired feedback control and tactile perception.

Ben Mitchinson was born in Cambridge, UK in 1975. He obtained BSc physics (1997), MSc control systems engineering (1998), and PhD in non-linear learning machines (2002) from the University of Sheffield, Sheffield, UK. Since then he has been working with the Adaptive Behaviour Research Group, also at Sheffield, on the WhiskerBot project. His research interests centre upon bio-inspired automation and learning systems.

Anthony G. Pipe is Deputy Director of the Bristol Robotics Laboratory and Reader in Robotics and Autonomous Systems. He received his PhD in 1997. He has 12 years experience of carrying out research in biologically-inspired robotics, machine learning and adaptive behavior, applied to intelligent and distributed control/monitoring systems. Although he is an electronics/control engineer, he works extensively with other engineers and life scientists, such as neurobiologists, neuroscientists and anatomists, since this is crucial to the forward advance of his work on modern robotics.

Chris Melhuish is Director of the Bristol Robotics Laboratory. He has degrees in geology from Durham University, an MSc in computer science from Bristol University and a PhD in collective robotics from the University of the West of England. He is a member of the British Computer Society and is a Chartered Engineer. His research interests include collective mobile robotics, robot–human interaction, neuro-inspired systems and energy autonomy in robots. In addition to his chair at the University of the West of England he also holds the chair in Robotics and Autonomous Systems at the University of Bristol.

Tony Prescott holds an MA in psychology (Edinburgh, 1984), an MSc in applied artificial intelligence (Aberdeen, 1989) and a PhD (Sheffield, 1994) on reinforcement and model-based learning. He is currently a senior lecturer in psychology at the University of Sheffield where he co-directs the department's Adaptive Behavior Research Group (http://www.abrg.group.shef.ac.uk/). His research interests are focused on understanding the functional architecture of the vertebrate brain using techniques in computational neuroscience, robotics, and neuroethology.